COMPDYN 2013
4th ECCOMAS Thematic Conference on
Computational Methods in Structural Dynamics and Earthquake Engineering
M. Papadrakakis, V. Papadopoulos, V. Plevris (eds.)
Kos Island, Greece, 12–14 June 2013

BEHAVIOUR OF A GEOSYNTHETIC REINFORCED STEEP SLOPE CONSTRUCTED WITH COHESIVE BACKFILL UNDER EARTHQUAKE LOADING

Castorina Silva Vieira[1] **and Maria de Lurdes Lopes**[1]

[1] University of Porto – Faculty of Engineering – Civil Engineering Department
R. Dr Roberto Frias, s/n 4200-465 Porto, Portugal
cvieira@fe.up.pt; lcosta@fe.up.pt

Keywords: Geosynthetics, Reinforced soil, Cohesive Soil, Numerical modelling, Earthquake loading

Abstract. *The use of geosynthetics as reinforcement elements of granular backfills has been widely used and their behaviour either during the service life or under seismic loading has been studied by several authors [1, 2]. However the use of fine grained soils, often referred as marginal fills, are not strongly implemented and, since they are susceptible for pore water pressure, not recommended by some international guidelines and standards. The use of soils locally available has cost benefits and sustainable gains. Therefore it is important to study the behaviour of geosynthetic reinforced steep slopes constructed with cohesive backfills.*

In this work the two-dimensional finite difference program Fast Lagrangian Analysis of Continua (FLAC) was used to model the seismic behaviour of an 8.4 m high geogrid-reinforced steep slope. The embankment was reinforced with 14 horizontal reinforcement layers and its face is inclined of 60º. The seismic behaviour of the structure constructed with cohesive backfill was compared to its behaviour if a granular material was selected.

Two constitutive models were used to model the cohesive backfills: the Mohr-Coulomb model and a Strain-Softening model.

In order to investigate the influence of input motion on the seismic behaviour of the structure, two earthquake ground motions artificially generated and two variable amplitude harmonic motions were considered.

The numerical simulations of the structure behaviour under seismic loading showed that the possible decrease of the backfill shear strength properties with the shear strain during cycling is an important issue. Even so, it could be concluded that a well compacted and drained cohesive soil can be used as backfill material in geosynthetic reinforced steep slopes.

1 INTRODUCTION

The use of geosynthetics as reinforcement elements of granular backfills has been widely used and their behaviour either during the service life or under seismic loading has been studied by several authors [1, 2]. However the use of fine grained soils, often referred as marginal fills, are not strongly implemented and not recommended by international guidelines and standards [3] since they are susceptible for pore water pressure.

Although there are several reasons for requiring good quality granular soils as backfill materials of reinforced earth structures, this specification could limit the use of these structures when these materials are not available near the site construction.

The use of poorly draining soils as backfill materials in geosynthetic reinforced structures brings some concerns, namely [4]:

- The pore water pressures induced during construction may reduce the backfill strength. Furthermore, the drained frictional strength of cohesive soils is lower than that of cohesionless soils;
- Post-construction movements may occur under sustained stresses as a result of the higher creep potential of poorly draining soils;
- Poorly draining soils are usually more difficult to compact.

These concerns may be mitigated since in many cases, the excess pore water pressures can be reduced by adopting suitable construction techniques and drainage systems. Some studies [5, 6] have shown that in many cases pore water pressure excesses are not generated and when the fill is compacted close to the optimum moisture content, the reinforced soil structure contains significant suctions (negative pore water pressures). Moreover, the use of some geosynthetics such as nonwoven geotextiles sheets has been reported to allow better compaction of cohesive soils [4, 7].

The use of soils locally available has cost benefits and sustainable gains. Therefore it is important to study the behaviour of geosynthetic reinforced steep slopes constructed with cohesive backfills.

The work herein presented is a preliminary study of the behaviour of geosynthetic reinforced steep slopes constructed with cohesive backfill. The effect of water content and pore water pressures will not be analyzed in this paper. The influence of some parameters, such as soil constitutive model, reinforcement stiffness and seismic input motion will be presented.

2 BRIEF DESCRIPTION OF FLAC CODE AND SEISMIC LOADING INPUT

FLAC is an explicit finite difference program that performs a Lagrangian analysis. The finite difference method is perhaps the oldest numerical technique used for the solution of sets of differential equations, given initial values and/or boundary values [8]. For dynamic analyses the full equations of motion are solved using lumped gridpoint masses derived from the real density of surrounding zones (rather than fictitious masses used for static solution). Each triangular sub-zone contributes one-third of its mass (computed from zone density and area) to each of the three associated gridpoints. The final gridpoint mass is then divided by two in the case of a quadrilateral zone that contains two overlays. In finite-element terminology, FLAC uses lumped masses and a diagonal mass matrix [8].

In FLAC, the dynamic input can be applied as an acceleration history, as a velocity history, as a stress (or pressure) history or as a force history. Dynamic input can be applied either in the x or y directions corresponding to the xy axes for the model, or in the normal and shear directions to the model boundary.

Two types of seismic action were considered in this study: two earthquake ground motions artificially generated and variable amplitude single frequency harmonic motions with identical peak ground acceleration. Two values of frequency were analyzed for the variable amplitude harmonic acceleration: 3 Hz, close to the fundamental frequency of the structure and 4 Hz.

Figure 1(a) presents one of the earthquake ground motions artificially generated [9] according to Portuguese National Annexes (PNA) of Eurocode 8 [10] for the greatest seismicity area of Portugal, considering seismic action type 2 (earthquake with moderate magnitude and small focal distance – close earthquake) and ground type B (deposits of very dense sand, gravel or very stiff clay). According to the PNA of Eurocode 8 [10] for the greatest seismicity area, the peak ground acceleration on type B ground is $2.7 m/s^2$ for a close earthquake (seismic action type 2). The duration of the stationary part of the accelerograms is equal to 10 seconds. The Fourier spectrum for the accelerogram presented in Figure 1(a) is plotted in Figure 1(b). This graph indicates that the highest frequency is less than approximately 20 Hz and that the majority of the frequencies are less than 13 Hz. Even so, before applying the seismic input motions, they were filtered to remove frequencies above the maximum frequency that can be modelled accurately.

Figure 2 illustrates the variable amplitude single frequency harmonic motions with frequency of 3 Hz.

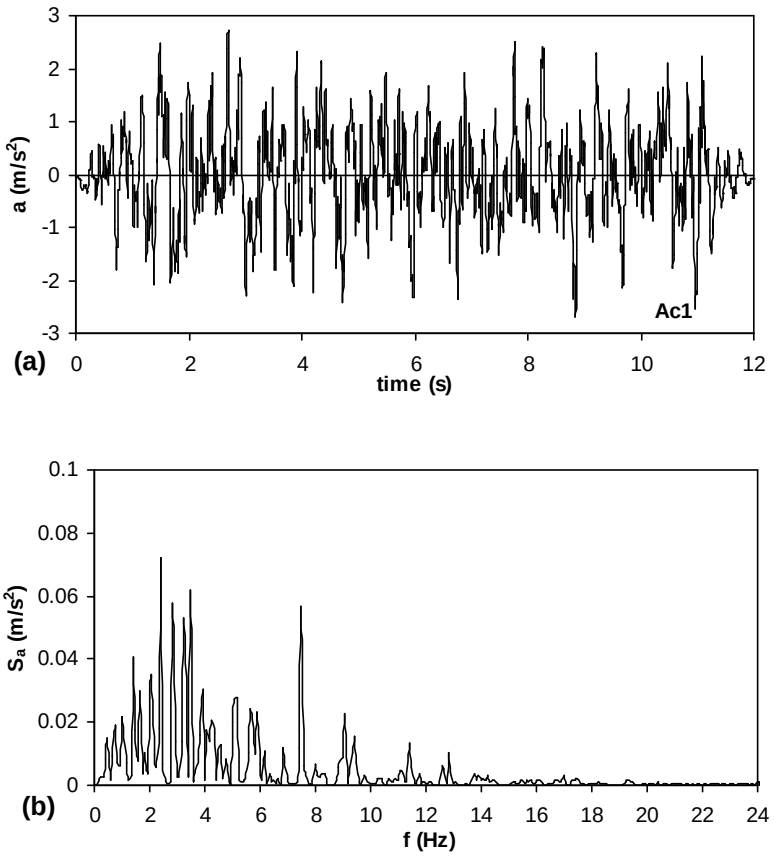

Figure 1: One seismic input motion used in this study: a) artificial accelerogram; b) Fourier spectrum.

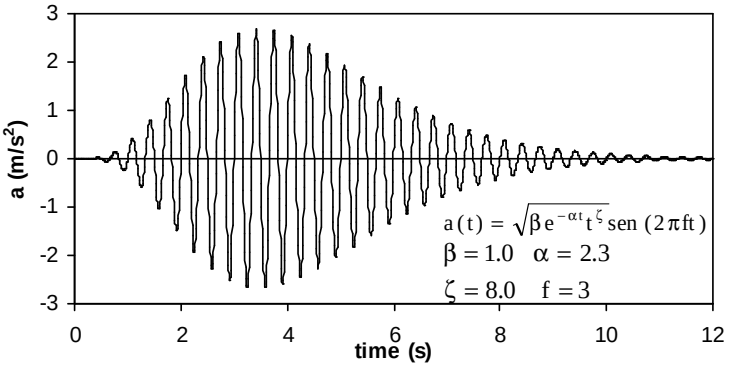

Figure 2: Variable amplitude single frequency harmonic motion (f = 3Hz).

In the analyses presented in this paper, two constitutive models were used: the *Mohr-Coulomb* model and a *Strain-Softening* model.

In the implementation of the *Mohr-Coulomb* model in FLAC, principal stresses σ_1, σ_2, σ_3 are used, being the out-of-plane stress, σ_{zz}, recognized as one of these. With the ordering convention $\sigma_1 \leq \sigma_2 \leq \sigma_3$ (compressive stresses are negative), the failure criterion for this model is represented in the plane (σ_1, σ_3) as illustrated in Figure 3.

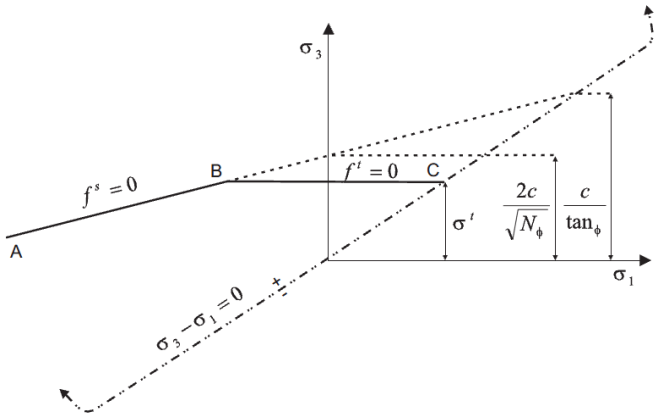

Figure 3: Mohr-Coulomb failure criterion in FLAC [8].

The failure envelope is defined from point A to point B (Figure 3) by the *Mohr-Coulomb* yield function:

$$f^s = \sigma_1 - \sigma_3 N_\phi + 2c\sqrt{N_\phi} \tag{1}$$

and from B to C by a tension yield function of the form:

$$f^t = \sigma^t - \sigma_3 \tag{2}$$

where ϕ is the soil friction angle, c is the cohesion, σ^t is the tensile strength and N_ϕ is defined as:

$$N_\phi = \frac{1+\sin\phi}{1-\sin\phi} \tag{3}$$

The tensile strength of the material, σ^t, cannot exceed the maximum value given by:

$$\sigma^t_{max} = \frac{c}{\tan\phi} \tag{4}$$

The *Strain-Hardening/Softening* model is based on the *Mohr-Coulomb* model with non-associated tension flow rules. The difference lies in the possibility that cohesion, friction, dilatation and tensile strength may harden or soften after the onset plastic yield [8]. The user can define the variation of the cohesion, friction and dilation as a function of the plastic shear strain. The variation of the tensile strength can also be prescribed in terms of plastic tensile strength. The code measures the total plastic shear and tensile strains at each timestep and causes the model properties to conform to the user-defined functions.

More details about these models and their implementation can be found in the manual of the software [8].

3 NUMERICAL GRID AND MATERIAL PROPERTIES

The geosynthetic reinforced embankment is 8.4 m high, reinforced with 14 horizontal reinforcement layers of length 6.8 m (L ≈ 0.8H) uniformly spaced and supported by a stiff foundation. The slope face is inclined of 60º. The geometry of the model and the numerical grid is illustrated in Figure 4.

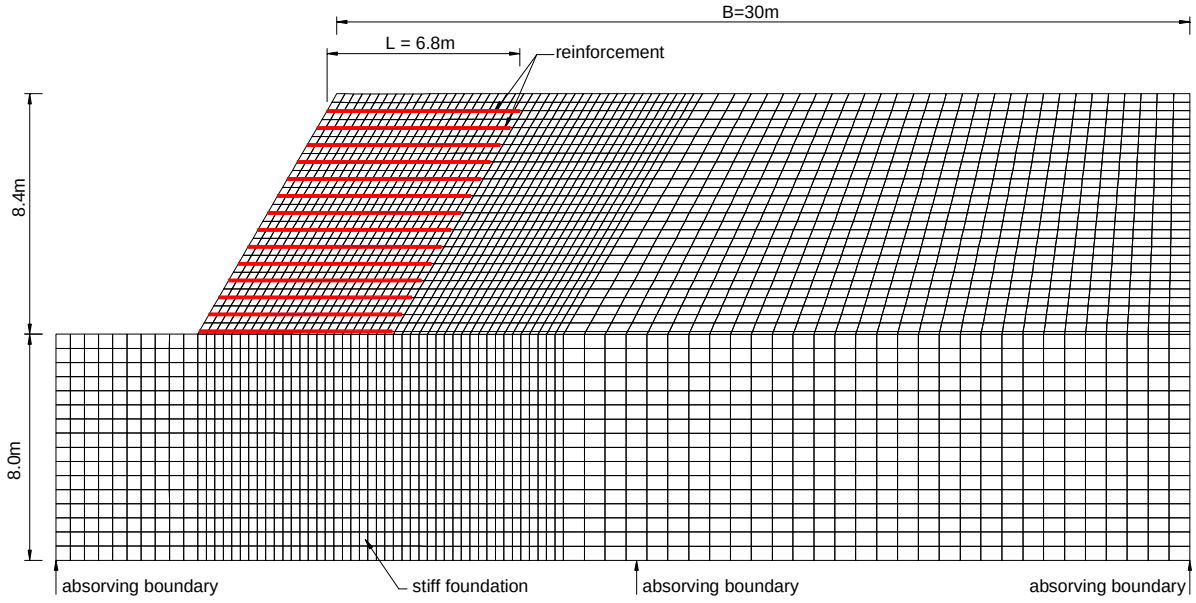

Figure 4: Geometrical properties and numerical grid.

The reinforcement layers were modelled using linear elasto-plastic cable elements with negligible compressive strength. The tensile yield strength was taken equal to 50 kN/m corresponding to the long term design strength (120 years) of a high strength composite geotextile, with nominal strength of 100 kN/m. The linear elastic stiffness of the reinforcement depends on the reinforcement strength and strain level. The reinforcement stiffness was taken equal to 1000 kN/m (approximately the stiffness value corresponding to 2% of strain). The influence of the reinforcement stiffness on the seismic behaviour of the structure is also analysed in this study.

The interface between the reinforcement and the soil was modelled by a grout material. The interface shear strength was considered dependent of the backfill shear strength.

A granular and two cohesive soils were considered as backfill material. Table 1 summarizes the soil properties. The granular soil was modelled as a purely frictional elasto-plastic material, with a *Mohr-Coulomb* yield function and a non-associated flow rule ($\psi = 0^o$). Two constitutive models were used to model the behaviour of the cohesive backfills: *Mohr-Coulomb* model and *Strain-Softening* model.

	Foundation	Granular Backfill	Cohesive Backfill "I"	Cohesive Backfill "II"
Unit weight, γ (kN/m^3)	22	17.5	16	16
Elasticity modulus, E (kN/m^2)	200×10^3	60×10^3	30×10^3	30×10^3
Poisson ratio, υ	0.30	0.30	0.30	0.30
Shear modulus, G (kN/m^2)	76.9×10^3	23.1×10^3	11.5×10^3	11.5×10^3
Cohesion, c (kN/m^2)	50	0	20	20
Internal friction angle, ϕ (^{o})	45	35	27	10

Table 1: Soil properties.

Figure 5 presents the variation of the internal friction angle and cohesion of the cohesive backfill "I", with the shear plastic strain, assumed in the *Strain-Softening* model. The values remain constant for shear plastic strains greater than 1%.

To analyze the importance of the backfill cohesion in the seismic behaviour of the reinforced embankment, a second situation was admitted: no variation of the backfill cohesion with shear plastic strain (thin line in Figure 5b - *Strain-Softening_f*) and the variation of the backfill friction angle shown in Figure 5(a).

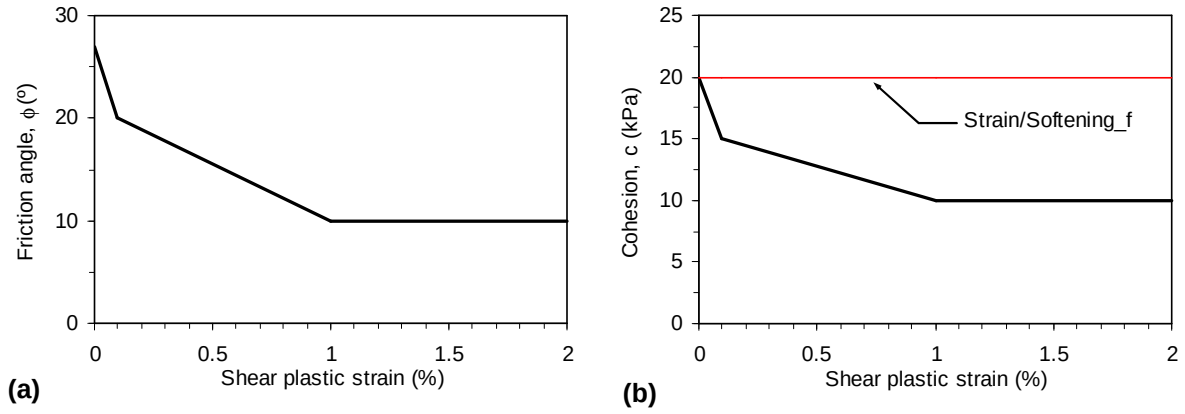

Figure 5: Decrease of backfill properties with shear plastic strains in the *Strain-Softening* model (cohesive backfill "I"): (a) internal friction angle, ϕ; (b) cohesion, c.

4 EFFECT OF BACKFILL SOIL

4.1 Influence of the constitutive model for cohesive backfill

After the simulation of the embankment construction with the cohesive backfill "I" (see Table 1) considering the *Strain-Softening* model and the shear strength decrease plotted in Figure 5, the structure was submitted to the artificial accelerogram plotted in Figure 1(a).

Based on the elastic properties of the soil and the mesh size, the maximum frequency that could be modelled accurately was 11.3Hz. So, before applying the seismic input, the frequencies above 10 Hz were removed. The filtered accelerogram was checked for the baseline drift (i.e., continuing residual displacement after the motion has finished) and a baseline correction was carried out [2].

Figure 6 shows the contours of horizontal displacements at the end of the seismic motion considering the embankment constructed with the cohesive backfill "I" and the *Strain-Softening* model (Figure 5). This figure indicates the imminent failure of the structure. The potential failure surface has developed in the retaining soil, i.e., behind the reinforced soil mass. The potential failure surface is also clear in Figure 7, where the maximum shear strain increments at the end of the seismic motion are represented.

Figures 6 and 7 show that if the backfill shear strength decreases significantly during the seismic motion, the stability of the reinforced embankment can be compromised.

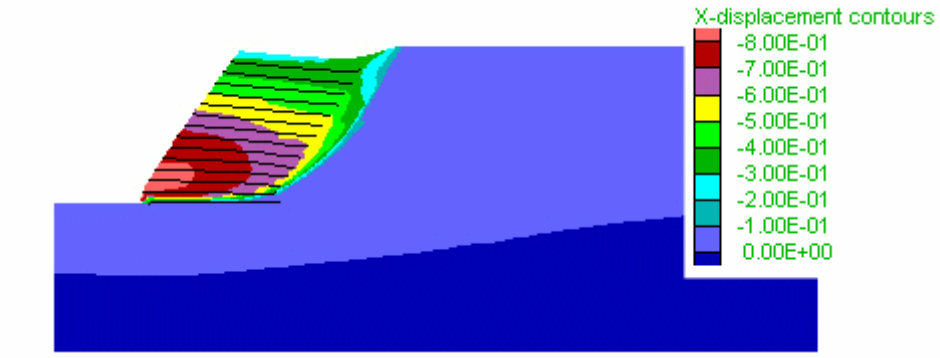

Figure 6: Contours of horizontal displacements at the end of the seismic motion considering the *Strain-Softening* model (cohesive backfill "I").

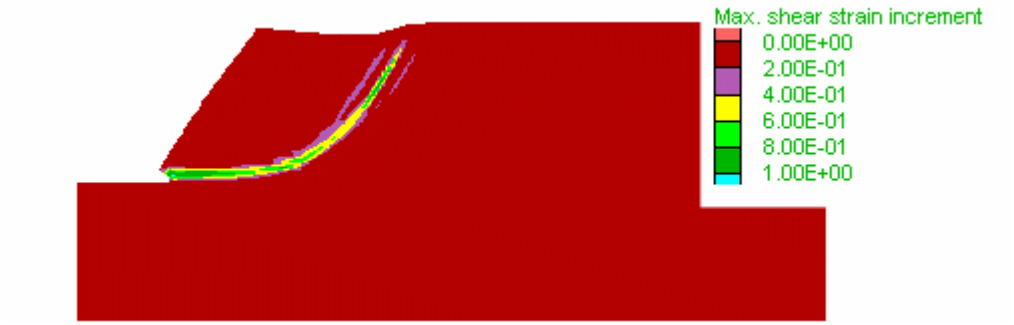

Figure 7: Maximum shear strain increments at the end of the seismic motion considering the *Strain-Softening* model (cohesive backfill "I").

As mentioned previously, to isolate the effect of the cohesive component it was performed an analysis in which only the backfill friction angle decreased with shear plastic strain. This analysis was referred as *Strain-Softening_f*. As expected, since the backfill shear strength is higher, this analysis has shown that at the end of the seismic motion the embankment deformation will be smaller. However, so large differences were not expected. For example, the decrease in the maximum residual horizontal displacement of the slope face was 95% and the maximum reinforcement tensile force decreases 68%.

Figure 8 compares the residual horizontal displacements of the slope face and the residual surface settlements at the end of the seismic motion, when the cohesive backfill was modelled by *Mohr-Coulomb* and *Strain-Softening* models. In the *Mohr-Coulomb* model the backfill shear properties are kept constant during the ground motion, so the embankment deformation is much smaller. It should be noted that in the *Strain-Softening* model only the decrease of the backfill friction angle was considered (model *Strain-Softening_f*).

Figure 8(a) evidences that when the *Strain-Softening* model was considered, the pattern of the horizontal displacements of the slope face underwent some changes. The displacements near the slope base tend to increase significantly.

The maximum reinforcement tensile loads obtained with the two models are illustrated in Figure 9. The differences in the reinforcement tensile loads are more significant in the lower half height of the embankment.

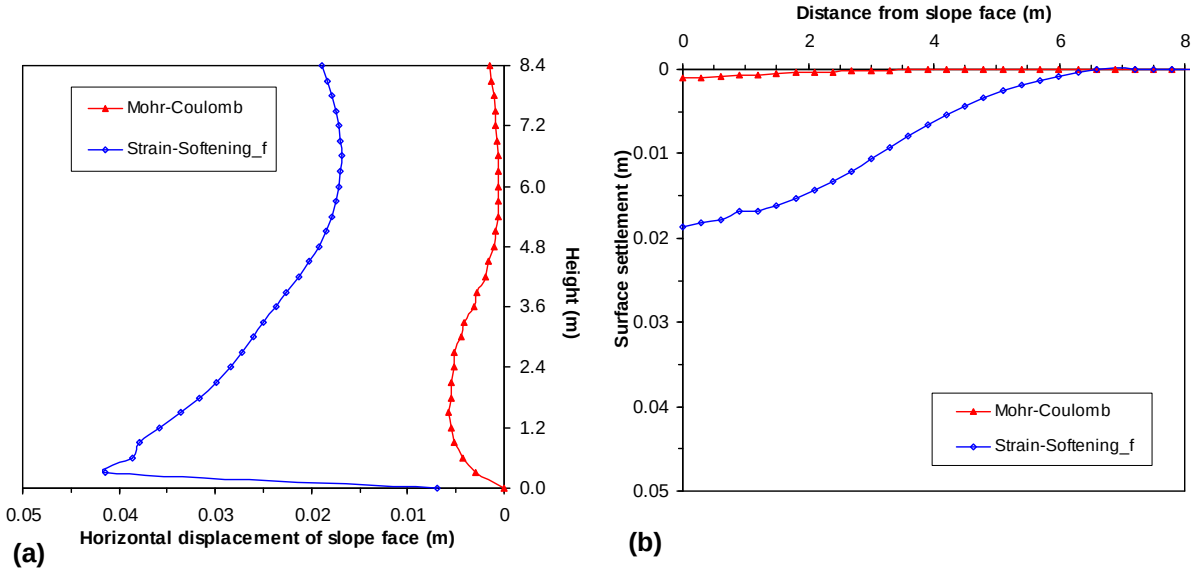

Figure 8: Effect of the backfill constitutive model on: (a) horizontal displacements of the slope face; (b) surface settlements.

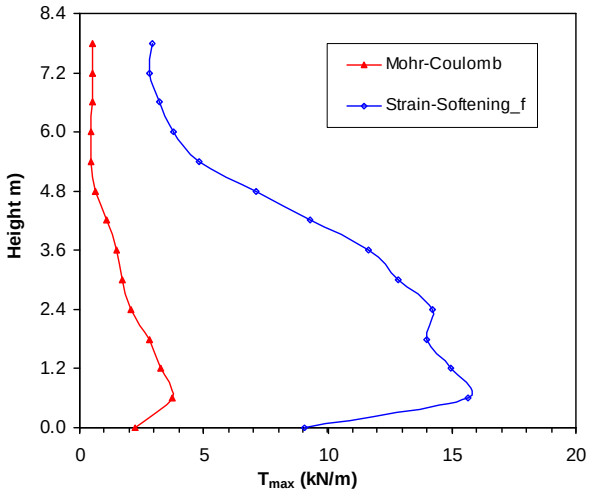

Figure 9: Effect of the backfill constitutive model on the maximum reinforcement tensile loads.

Figures 8 and 9 show that the decrease of the backfill friction angle with the shear strain (Figure 5a) is an important factor in the seismic behaviour of the structure. The conclusions presented by some researchers regarding the good behaviour of reinforced soil walls constructed with cohesive backfills should be regarded with some reserves.

The cohesive backfill "II" was selected to have the same shear strength properties of the backfill "I" when the *Strain-Softening_f* is assumed and the shear plastic strain exceeds 1% (see Table 1 and Figure 5).

Figure 10 compares the residual horizontal displacements of the slope face and the maximum reinforcement tensile loads obtained for the cohesive backfill "I", modelled with the *Strain-Softening_f* model, with the results obtained for the cohesive backfill "II", analyzed with the *Mohr-Coulomb* model.

Taking into consideration that the cohesive component is equal for both backfills, Figure 10 illustrates the influence of the frictional component of the backfill. Note that the friction angle is also the same for shear plastic strains greater than 1%.

For the cohesive backfill "II", the friction angle is equal to 10º throughout the numerical simulation so, greater residual deformations were expected. However, Figure 10(b) shows that the differences in the maximum reinforcement tensile loads were not very significant. Greater reinforcement tensile loads were achieved for most of the layers when cohesive backfill "I" was admitted.

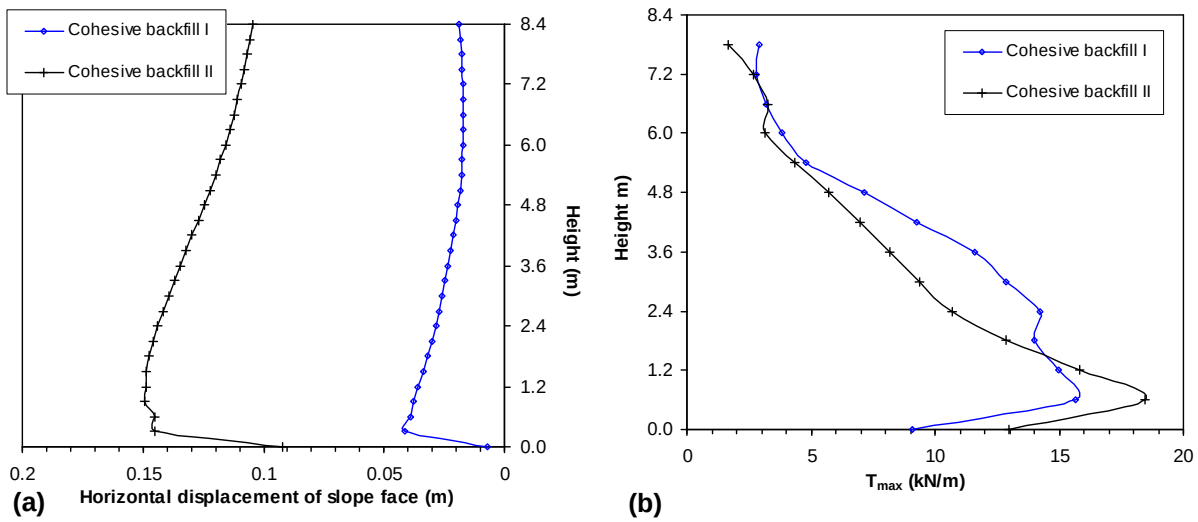

Figure 10: Influence of the frictional component of the backfill on: (a) horizontal displacement of the slope face; (b) the maximum reinforcement tensile loads.

4.2 Effect of backfill soil type

The influence of the backfill soil properties on the residual horizontal displacements of the slope face and maximum reinforcement tensile loads is illustrated in Figure 11. The granular backfill and the cohesive backfill "II" were analyzed with the *Mohr-Coulomb* model. The cohesive backfill "I" was modelled by the *Strain-Softening_f* model (see Figure 5).

The theoretical distribution of the reinforcement tensile forces considering the granular backfill, the horizontal seismic coefficient, k_h, equal to 0.27 and the seismic earth pressure coefficients estimated by the equation proposed by [11] is also plotted in Figure 11(b).

Figure 11(a) shows that the residual horizontal displacements of the slope face for the embankment constructed with the granular backfill are, in general, between the values achieved for the cohesive backfills. As mentioned, the displacements near the slope base increase when the *Strain-Softening* model is used.

For the same constitutive model (*Mohr-Coulomb*), greater reinforcement tensile loads were achieved in the embankment constructed with the granular backfill (with exception of the 3 lower reinforcement layers). If the embankment has been constructed with the cohesive backfill "I" and modelled with the *Strain-Softening_ f* model, the maximum reinforcement tensile loads in the lower half of the embankment height exceed the tensile loads achieved for the granular backfill (Figure 11b).

For the granular backfill, the maximum reinforcement tensile loads for the layers located in the upper half height of the embankment are very close to those estimated by the theoretical distribution (with the exception of the top layers, where the theoretical distribution underestimates the reinforcement tensile loads). The theoretical distribution overestimates the reinforcement tensile loads for the reinforcement layers located in the lower half of the embankment height.

It can be seen in Figure 11(b) that the maximum reinforcement tensile load recorded in the 4th reinforcement layer was not very different when distinct backfill materials were used. Notwithstanding, the distribution of the tensile forces (and consequently, the axial strain) through the reinforcement length can be different. Figure 12 illustrates the axial strains through the reinforcement length of the 4th layer obtained for the three backfill materials.

The sudden decrease of the axial strain near the end of the reinforcement for the cohesive backfill "II" suggests that the reinforcement length could not be the appropriate. Even if the maximum axial strain reached in the three simulations has been similar, the axial strain distribution when the *Strain-Softening_ f* model was used (cohesive backfill "I") was significantly distinct from those achieved with the *Mohr-Coulomb* model.

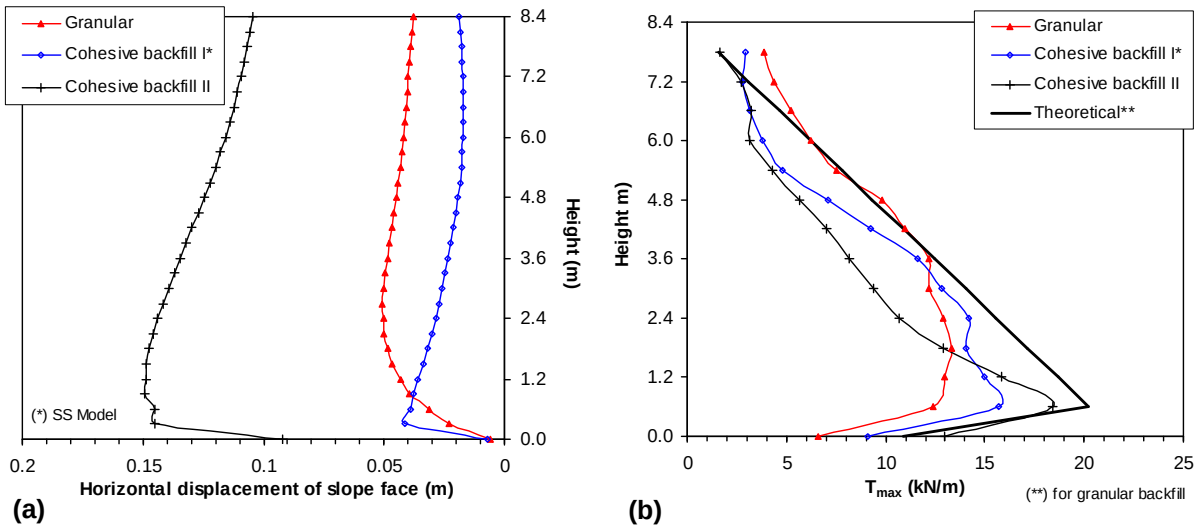

Figure 11: Influence of the backfill soil properties on: (a) horizontal displacement of the slope face; (b) the maximum reinforcement tensile loads.

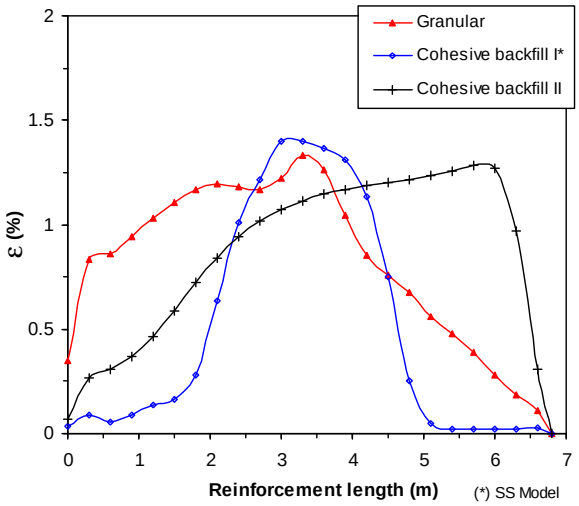

Figure 12: Influence of the backfill soil properties on the axial strain through the 4th reinforcement layer.

5 INFLUENCE OF INPUT MOTION

In order to investigate the influence of the input motion on seismic behaviour of the structure, as it was referred in section 2, four input motions were considered: two earthquake ground motions artificially generated and two variable amplitude single frequency harmonic motions, with frequencies of 3Hz (close to the fundamental frequency of the structure) and 4 Hz.

Figure 13 presents the effect of the seismic input motion on the residual horizontal displacements of the slope face and on the maximum reinforcement tensile loads. The variable amplitude harmonic motion with frequency of 3 Hz induces, not unexpectedly, very large lateral displacements and reinforcement tensile loads. It should be remembered that this frequency is close to the fundamental frequency of the structure. This input motion is much more aggressive to the structure than the earthquake loadings. On the other hand, the residual deformations recorded at the end of the harmonic motion with frequency of 4 Hz are not significantly different from those obtained with the earthquake loadings.

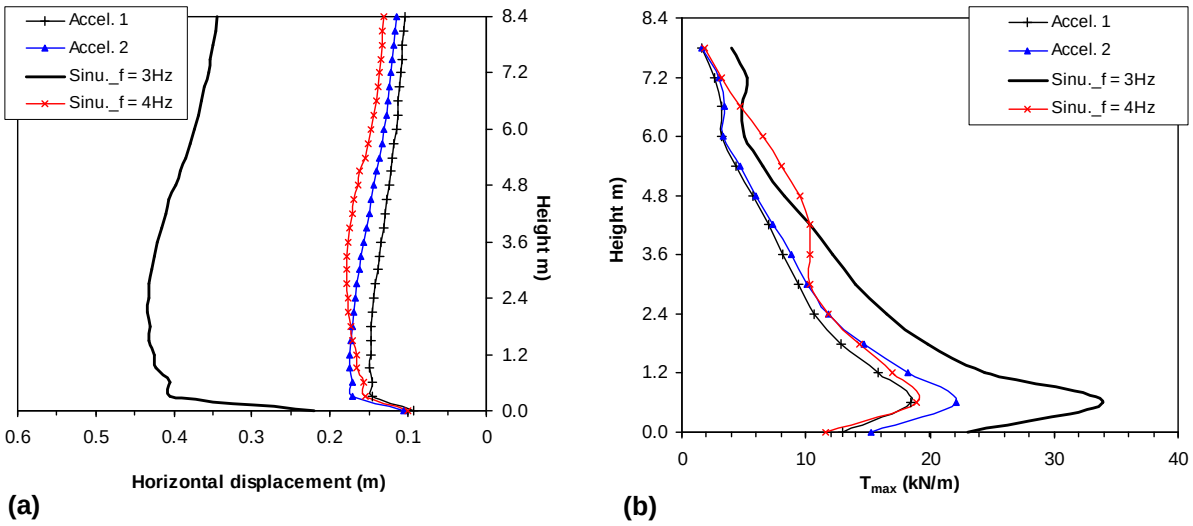

Figure 13: Influence of the seismic input motion on: (a) horizontal displacement of the slope face; (b) the maximum reinforcement tensile loads.

Figure 14 illustrates the time histories of the tensile load recorded 2 m from the slope face in the 2nd reinforcement layer. This graph shows that, for the harmonic motion with f = 3Hz the tensile load increased almost fourteen times, when compared to the value installed at begin of the input motion. In particular for the harmonic motions, the tensile load variation after 6 seconds was very small. The variations induced by the earthquake motions were gentler.

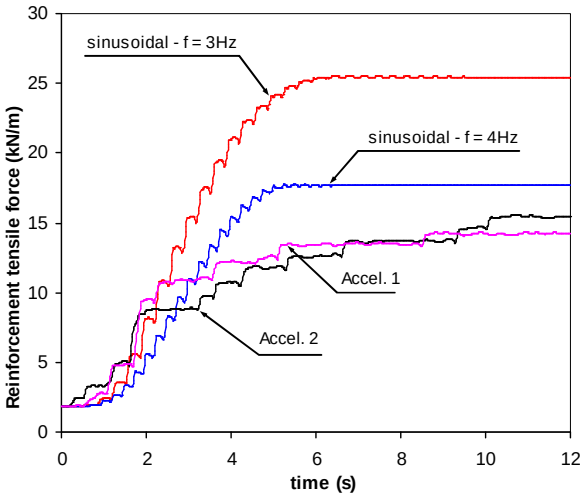

Figure 14: Time histories of the tensile loads recorded at 2 m from the slope face in the 2nd reinforcement layer.

6 EFFECT OF REINFORCEMENT STIFFNESS

The effect of the reinforcement stiffness on the seismic behaviour of the reinforced embankment constructed with the cohesive backfill "II" was analyzed. Figure 15 shows the residual horizontal displacements of the slope face and reinforcement tensile loads for three geosynthetics: a geotextile (J = 250 kN/m), a low strength geogrid (J = 500kN/m) and a medium strength geogrid or a high strength composite geotextile (J = 1000kN/m). These values were estimated for 2% of strain.

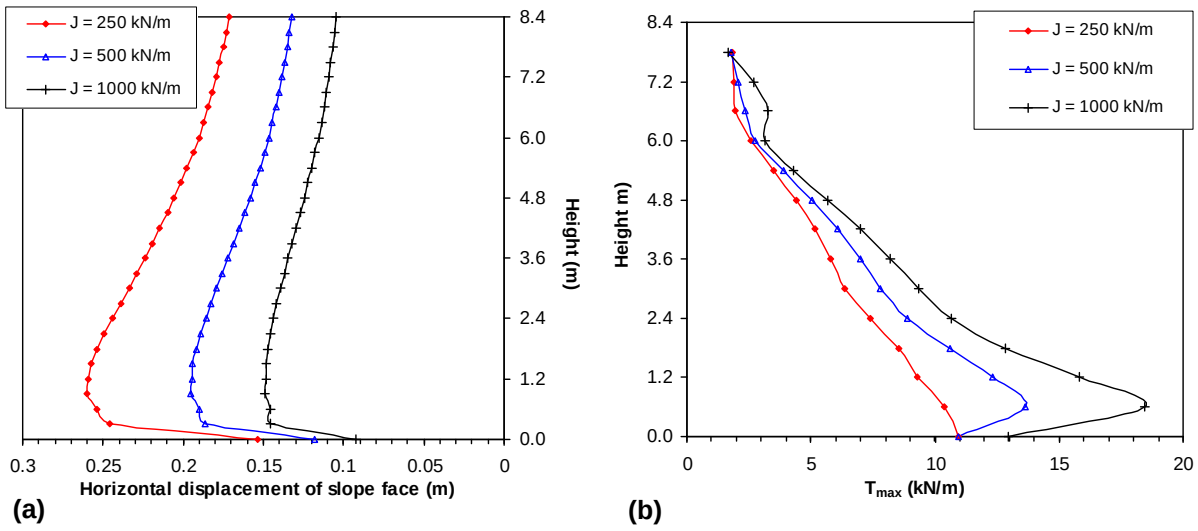

Figure 15: Influence of the reinforcement axial stiffness on: (a) horizontal displacement of the slope face; (b) the maximum reinforcement tensile loads.

Not unexpectedly, the residual deformations of the slope face increased with the decrease of the reinforcement stiffness (Figure 15a).

The stiffer reinforcements have been subjected to greater reinforcement tensile loads. For the lower value of the reinforcement stiffness, the restraining effect of the foundation (which causes small tensile load in the lower reinforcement layer) disappeared (Figure 15b).

7 CONCLUSIONS

The use of soils locally available has cost benefits and sustainable gains. Therefore it is important to study the behaviour of geosynthetic reinforced steep slopes constructed with cohesive backfills.

This numerical study carried out allows drawing the following main conclusions:

- If the backfill shear strength decreases significantly during the seismic motion, the stability of the reinforced embankment can be compromised.
- When the *Strain-Softening* model was used, the residual displacements near the slope base tended to increase significantly.
- The decrease of the backfill friction angle with the shear strain is an important factor in the seismic behaviour of the structure. The conclusions presented by some researchers regarding the good behaviour of reinforced soil walls constructed with cohesive backfills should be regarded with some reserves.
- Single frequency harmonic motions may be useful to analyse the dynamic response of reinforced soil structures, however the magnitude of the response might be excessive when compared to artificial (or real) earthquake ground motions.

The numerical study herein presented has some limitations, namely, neglecting the effect of water content and pore water pressures. Even so, the achieved results indicate that the use of cohesive soils as backfill material of geosynthetic reinforced steep slopes can have advantages and encourage further research.

ACKNOWLEDGMENTS

The authors would like to thank the financial support of Portuguese Science and Technology Foundation (FCT) and FEDER, Research Project FCOMP-01-0124-FEDER-009750 - PTDC/ECM/100975/2008.

REFERENCES

[1] Bathurst, R.J., Hatami, K. Seismic response analysis of a geosynthetic-reinforced soil retaining wall. *Geosynthetics International*, **5**(1-2), pp. 127-166, 1998.

[2] Vieira, C.S., Lopes, M.L., Caldeira, L.M. Numerical modelling of a geosynthetic reinforced steep slope subjected to seismic loading. *Proc. of 3rd Computational Methods in Structural Dynamics and Earthquake Engineering - COMPDYN 2011*, Corfu, Greece, 2011.

[3] BS 8006. Code of practice for strengthened/reinforced soils and other fills, in British Standard Institution, 260p, 2010.

[4] Zornberg, J.G., Mitchell, J.K. Reinforced soil structures with poorly draining backfills. Part I: reinforcement interactions and functions. *Geosynthetics International*, **1**(1), pp. 103–147, 1994.

[5] Liu, Y., Scott, J.D., Sego, D.C. Geogrid reinforced clay slopes in a test embankment. *Geosynthetics International*, **1**(1), pp. 67-91, 1994.

[6] Dobie, M. Practical use of clay fills in reinforced soil structures. *Development of Geotechnical Engineering in Civil Works and Geo-Environment*, Yogyakarta, December 2010.

[7] Mitchell, J.K., Zornberg, J.G. Reinforced soil structures with poorly draining backfills. Part ii: case histories and applications. *Geosynthetics International*, **2**(1), pp. 265–307, 1995.

[8] Itasca. FLAC - Fast Lagrangian Analysis of Continua, Version 5.00, Itasca Consulting Group, Inc., USA, 2005.

[9] Gasparini, D., Vanmarcke, E. SIMQKE - A computer program for artificial motion generation, in User's Manual and Documentation, Department of Civil Engineering, Massachusetts Institute of Technology, 1976.

[10] [NP-ENV 1998-1-1. Eurocode 8: Design provisions for earthquake resistance of structures. Part 1-1: General rules – Seismic actions and general requirements for structures. Portuguese NAD, 2010.

[11] Vieira, C.S., Lopes, M.L., Caldeira, L.M. Earth pressure coefficients for design of geosynthetic reinforced soil structures. *Geotextiles and Geomembranes*, **29**(5), pp. 491-501, 2011.